Proceedings of the 2015
IEEE Conference on Robotics and Biomimetics
Zhuhai, China, December 6-9, 2015

An RBF-Based Neuro-Adaptive Control Scheme to Drive a Lower Limb Rehabilitation Robot

Chengkun Cui, Gui-Bin Bian, Zeng-Guang Hou, Min Tan, Dongxu Zhang, Xiao-Liang Xie, Weiqun Wang

Abstract— **In this paper, a novel robust adaptive control scheme is proposed for a lower limb rehabilitation robot designed by our laboratory. The proposed control strategy is based on the radial basis function (RBF) neural networks and the parameters of the system dynamics are unknown. The weights of the RBF neural networks are updated by an adaptive law according to the Lyapunov stability analysis. The robustness against possible variations of the system dynamics and the external disturbance are considered in the control design. The proposed control strategy can not only avoid the complex procedure of system parameters identification, but also guarantee high robustness, small trajectory tracking errors and the assistance of the patient's voluntary participation. Using this control algorithm, the robot can regulate its exerted torque to adapt to the patient's active torque in real time during rehabilitation. The effectiveness of our control method is demonstrated by a simulation.**

I. Introduction

There have been an increasing number of patients suffered from neurologic damage in the world. Spinal cord injury, stroke and muscle weakness are common neurologic injuries which may seriously impair the patients' limb motion ability in the daily life [1]. Rehabilitation exercises can help the patients to restore the motor function to some extent. Traditional rehabilitation training methods are that therapists move the patients' paralyzed limbs repetitively by hand or simple devices, which are toilsome and time-consuming [2].

Different from the traditional rehabilitation, robotic technologies have shown superiority in providing more efficient and comfortable rehabilitation exercises. In recent years, rehabilitation robots are designed for conducting or assisting patients with hemiplegia or paraplegia to carry out repetitive rehabilitation training. The RoboKnee developed by Florida University is used to help the motion-impaired people to do the lower extremity locomotion training at the knee joint level [3]. The MotionMaker designed by SWRTEC is a reclining type lower limb rehabilitation robot [4]. The patient's hip, knee and ankle joints can be trained simultaneously with the help of the MotionMaker. The Lokomat which is developed by Hocoma is composed of a treadmill, a couple of gait orthoses and a weight reduction system [5]. It can conduct patient to carry out lower limb gait rehabilitation exercises. The Hybrid Assistive Limb-5 (HAL-5) is a wearable lower extremity exoskeleton robot which is designed by the University of Tsukuba [6]. The HAL-5 can assist the disabled to accomplish upper or lower extremity daily activities. Generally speaking, every rehabilitation robot has a control strategy enabling it to execute the rehabilitation exercises desired by the patients who use it. The patients can behave passive or generate either assistive or resistive torques during the actual rehabilitation training. Taking into account the complex dynamic changes from the patients' desired motion, the precise dynamics model of the human-robot hybrid system will hardly be established and the classical controllers (such as PID controllers) may probably get failed in this situation [7]. Some works based on the dynamics parameters identification of the human-robot hybrid system are put forward in recent literature [8], [9]. These methods can be valid only when the rehabilitation robot is used by the same patient in an invariant environment [10]. However, considering the morphology differences caused by different patients and the external environment disturbance, the parameters identification methods may be inaccuracy and time-consuming. In our previous work [11]–[15], in order to implement accurate objective tracking tasks of robot manipulators, different control schemes based on adaptive neural network are developed. This paper extends our adaptive control researches to the domain of rehabilitation robots. In this work, an RBF-based neuro-adaptive control strategy is put forward for a lower limb rehabilitation robot which is designed by our laboratory. A sliding mode robust term [16], [17] is introduced to our control design to improve anti-interference capability. The proposed control strategy can not only avoid the complex process of system parameters identification, but also ensure good performance of the system, such as stability, robustness, trajectory tracking accuracy and the help of patients' voluntary participation. The remainder of the paper is organized as follows: section II introduces the human-robot hybrid system for lower limb rehabilitation and the detection method of the human voluntary motion. Section III presents the RBF-based neuro-adaptive control scheme and analyzes the system stability. The simulation and discussion of the control strategy are proposed in the Section IV. Section V gives the conclusion and future works.

II. Human-robot hybrid system and detection of human torque

The lower limb rehabilitation robot designed by our laboratory has 3-DOF (degree of freedom) corresponding

*This work is supported by the National Natural Science Foundation of China (Grants 61421004, 61225017, 61175076, 61203342) and Beijing Natural Science Foundation (Grant 4132077).

Chengkun Cui, Gui-Bin Bian, Zeng-Guang Hou, Min Tan, Dongxu Zhang, Xiao-Liang Xie, Weiqun Wang are with the State Key Laboratory of Management and Control for Complex Systems, Institute of Automation, Chinese Academy of Sciences, Beijing 100190, China. {cuichengkun2014, guibin.bian, zengguang.hou, min.tan, dongxu.zhang, xiaoliang.xie, weiqun.wang}@ia.ac.cn.

978-1-4673-9675-2/15/$31.00 © 2015 IEEE

to hip, knee and ankle joint, respectively. The mechanical structure of the robot is shown in Fig. 1. Torque sensors and encoders are installed to obtain the torques, angular positions and angular velocities of each joint. In the procedure of the rehabilitation exercises, the subject's thigh and crus are attached to the robot links and the foot is fastened to the pedal. Therefore the robot combined with the human lower limb can be viewed as a three-link structure. For the sake of simplicity, the mass of the whole system is assumed to be evenly distributed and the ankle joint is assumed to keep horizontal because it has few effects on the end trajectory. Thus, the simplified human-robot hybrid model can be regarded as a mass-evenly two-link system under the above assumptions. Fig. 2 shows the simplified model structure, where m_1 represents the total mass of robot link 1 and human thigh, m_2 denotes the total mass of robot link 2 and human crus, l_1 and l_2 are the length of link 1 and link 2, q_1 and q_2 are the actual angular position of the joint 1 (hip joint) and joint 2 (knee joint).

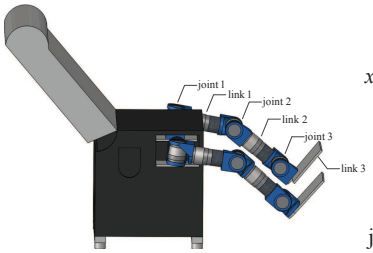

Fig. 1. Mechanical structure of the lower limb rehabilitation robot

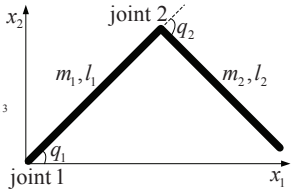

Fig. 2. Simplified model structure

The actual output torque of the human-robot hybrid system at every joint consists of two parts: the torque exerted by the robot and the torque generated by the human. The relationship between them can be represented as follows

$$\tau = \tau_r + \tau_h \tag{1}$$

where τ is the actual output torque, τ_r denotes the torque applied by the robot and τ_h represents the torque generated by the subject. The detection of the torque exerted by the subject is critical because it will have great effects on the torque produced by the robot motor. During training, the pedal is assumed to maintain horizontal. Thus, the actual output force of the pedal will be vertical with the ground all the time. The reading on the force sensor of the pedal will only be generated by the human leg gravity under the situation that no active force is applied by the subject. The link 1 and link 2 can supply the support force against the gravity of human leg at this time. The relationship between them can be deduced as follows

$$F_s = \frac{\frac{1}{2}m_t g l_1 \cos q_1 + m_c g[\frac{1}{2}l_2 \cos(q_1+q_2) + l_1 \cos q_1]}{l_1 \cos q_1 + l_2 \cos(q_1+q_2)} \tag{2}$$

where m_t denotes the mass of human thigh, m_c represents the mass of human crus, and F_s is the reading on the force sensor of the pedal at static status. We can calculate the human voluntary torque by using the deviation between F_s and the changing reading on the force sensor when the subject applies voluntary force to the pedal. The calculation formula can be written as [18]

$$\tau_h = \begin{bmatrix} (F_s - F) l_1 \sin(q_1+q_2) \sin q_2 \\ (F_s - F) l_2 \cos(q_1+q_2) \end{bmatrix}. \tag{3}$$

III. Control Design and Stability Analysis

As it is difficult to directly design a control law for the robot torque under the influence of the human active participation, we decide to design a novel and efficient control method for the actual output toque of the whole system. Considering the human voluntary torque can be detected using the method mentioned before, the robot torque can be calculated by using (1). In order to implement the performance that the robot can adaptively compensate to the patient's different voluntary efforts, a robust adaptive control law will be designed for the actual output torque. The dynamics model structure of human-robot hybrid system can be described as [19]

$$M(q)\ddot{q} + C(q,\dot{q})\dot{q} + G(q) + F(\dot{q}) + \tau_d = \tau \tag{4}$$

where $M(q)$ is the inertia matrix, $C(q,\dot{q})$ is the coriolis/centripetal matrix, $\dot{M}(q) - 2C(q,\dot{q})$ is a skew-symmetric matrix, $G(q)$ is the gravity vector, $F(\dot{q})$ is the friction vector, τ ($\tau = \tau_r + \tau_h$) is the actual output torque of the whole system, and τ_d is the unknown external disturbance which satisfies $\|\tau_d\| \leq \rho_d$.

Define the tracking error as follows

$$e = q_d - q \tag{5}$$

where q_d is the expected joint angular position and q is the actual joint angular position.

Define the filtered tracking error by the sliding mode transformation

$$r = \dot{e} + \Lambda e \tag{6}$$

where $\Lambda = \Lambda^T = diag(\lambda_1, \lambda_2, \cdots, \lambda_n)$, $\lambda_i > 0 (i = 1, \ldots, n)$. e and $\dot{e}$ converge exponentially (asymptotically) to zero when r converges exponentially (asymptotically) to zero [20].

Set

$$\dot{q}_r = r + \dot{q} \tag{7}$$

so we can get

$$\ddot{q}_r = \dot{r} + \ddot{q} \tag{8}$$

Substituting (7) and (8) into (4), we have

$$M\dot{r} = -Cr - \tau + f + \tau_d \tag{9}$$

where $f = M\ddot{q}_r + C\dot{q}_r + G + F$ and f contains the whole modeling information.

However, considering the human voluntary efforts and the external environment disturbance, the human-robot dynamics modeling is very difficult to obtain. Thus, our goal is to design an adaptive robust controller for the system without

any knowledge of the dynamics model parameters. To this end, we select a neural network adaptive control law as [21]

$$\tau = \hat{f} + K_v r \tag{10}$$

where $\hat{f}$ is an approximation of f, which can be generated by using RBF neural networks, $K_v = K_v^T > 0$ is a gain matrix. The control structure block diagram of the whole system is shown in Fig. 3.

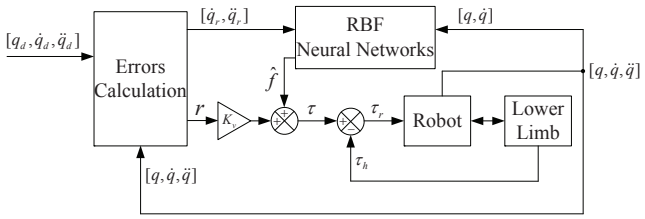

Fig. 3. Control structure block diagram

An RBF neural network with one hidden layer can be described as

$$y = W^T \varphi \tag{11}$$

where W is the weight matrix, $\varphi = [\phi_1 \ \phi_2 \ \cdots \ \phi_n]$ is the vector composed of basis functions, $\phi_i = \exp(-\|x - \mu_i\|^2 / 2\sigma_i^2)$ is the basis function of node i ($i = 1, 2, \cdots, n$), n is the number of nodes in the hidden layer. In order to get a high approximate accuracy, we choose four RBF neural networks to reconstruct $M(q)$, $C(q, \dot{q})$, $G(q)$, $F(\dot{q})$, respectively. This neural network approximation approach can also be used in many other fields, such as piezoelectric actuators [22]. The structure of the four RBF neural networks is shown in Fig. 4.

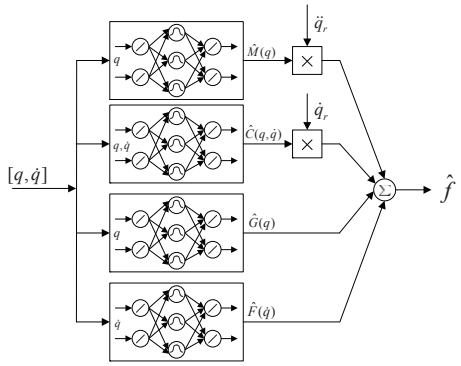

Fig. 4. Structure of the four RBF neural networks

Assume that the optimal outputs of four RBF neural networks are $M^*(q)$, $C^*(q, \dot{q})$, $G^*(q)$, $F^*(\dot{q})$, respectively.

$$\begin{aligned} M^*(q) &= W_M^{*T} \varphi_M \\ C^*(q, \dot{q}) &= W_C^{*T} \varphi_C \\ G^*(q) &= W_G^{*T} \varphi_G \\ F^*(q) &= W_F^{*T} \varphi_F \end{aligned} \tag{12}$$

where W^* is the optimal weight constant matrix that satisfies $\|W^*\|_F \leq W_{\max}$.

Define the optimal approximation error of the RBF neural networks as ε,

$$\varepsilon = f - f^* \tag{13}$$

and assume that ε satisfies $\|\varepsilon\| \leq \delta$.
The actual outputs of four RBF neural networks can be denoted as

$$\begin{aligned} \hat{M}(q) &= \hat{W}_M^T \varphi_M \\ \hat{C}(q, \dot{q}) &= \hat{W}_C^T \varphi_C \\ \hat{G}(q) &= \hat{W}_G^T \varphi_G \\ \hat{F}(q) &= \hat{W}_F^T \varphi_F \end{aligned} \tag{14}$$

Define the weight estimation errors as

$$\tilde{W} = W^* - \hat{W} \tag{15}$$

In order to resist the modeling errors and unknown external disturbance, we modify the adaptive control law (10) as follows

$$\tau = \hat{f} + K_v r - \xi \tag{16}$$

where ξ is a robust term which can be designed as $\xi = -(\delta + \rho_d) sgn(r)$.
By substituting (12)-(16) into (9), the closed-loop tracking filtered error dynamics can be expressed as

$$\begin{aligned} M\dot{r} &= -(K_v + C)r + \tilde{W}_M^T \varphi_M \ddot{q}_r + \tilde{W}_C^T \varphi_C \dot{q}_r \\ &\quad + \tilde{W}_G^T \varphi_G + \tilde{W}_F^T \varphi_F + \varepsilon + \tau_d + \xi \end{aligned} \tag{17}$$

The adaptation law of these weight matrices can be deduced according to the Lyapunov stability analysis [23].

$$\begin{aligned} \dot{\hat{W}}_M &= \Gamma_M \varphi_M \ddot{q}_r r^T - k_M \|r\| \Gamma_M \hat{W}_M \\ \dot{\hat{W}}_C &= \Gamma_C \varphi_C \dot{q}_r r^T - k_C \|r\| \Gamma_C \hat{W}_C \\ \dot{\hat{W}}_G &= \Gamma_G \varphi_G r^T - k_G \|r\| \Gamma_G \hat{W}_G \\ \dot{\hat{W}}_F &= \Gamma_F \varphi_F r^T - k_F \|r\| \Gamma_F \hat{W}_F \end{aligned} \tag{18}$$

where Γ_M, Γ_C, Γ_G, Γ_F are symmetric positive definite constant matrices and $k_M > 0$, $k_C > 0$, $k_G > 0$, $k_F > 0$.

To analyze the system stability, we construct a Lyapunov function as follows

$$\begin{aligned} V &= \frac{1}{2} r^T M r + \frac{1}{2} tr(\tilde{W}_M^T \Gamma_M^{-1} \tilde{W}_M) \\ &\quad + \frac{1}{2} tr(\tilde{W}_C^T \Gamma_C^{-1} \tilde{W}_C) + \frac{1}{2} tr(\tilde{W}_G^T \Gamma_G^{-1} \tilde{W}_G) \\ &\quad + \frac{1}{2} tr(\tilde{W}_F^T \Gamma_F^{-1} \tilde{W}_F) \end{aligned} \tag{19}$$

Calculating the time derivative of V,

$$\begin{aligned} \dot{V} &= r^T M \dot{r} + \frac{1}{2} r^T \dot{M} r + tr(\tilde{W}_M^T \Gamma_M^{-1} \dot{\tilde{W}}_M) \\ &\quad + tr(\tilde{W}_C^T \Gamma_C^{-1} \dot{\tilde{W}}_C) + tr(\tilde{W}_G^T \Gamma_G^{-1} \dot{\tilde{W}}_G) \\ &\quad + tr(\tilde{W}_F^T \Gamma_F^{-1} \dot{\tilde{W}}_F) \end{aligned} \tag{20}$$

By using (17) and considering $\dot{M}-2C$ is a skew-symmetric matrix, we can get

$$\begin{aligned}\dot{V} &= -r^T K_v r + tr(\tilde{W}_M^T(\Gamma_M^{-1}\dot{\tilde{W}}_M + \varphi_M \ddot{q}_r r^T)) \\ &\quad + tr(\tilde{W}_C^T(\Gamma_C^{-1}\dot{\tilde{W}}_C + \varphi_C \dot{q}_r r^T)) \\ &\quad + tr(\tilde{W}_G^T(\Gamma_G^{-1}\dot{\tilde{W}}_G + \varphi_G r^T)) \\ &\quad + tr(\tilde{W}_F^T(\Gamma_F^{-1}\dot{\tilde{W}}_F + \varphi_F r^T)) \\ &\quad + r^T\varepsilon + r^T\tau_d + r^T\xi\end{aligned} \tag{21}$$

Substituting (15) and (18) into (21), we have

$$\begin{aligned}\dot{V} &= -r^T K_v r + k_M \|r\| tr(\tilde{W}_M^T(W_M^* - \tilde{W}_M)) \\ &\quad + k_C \|r\| tr(\tilde{W}_C^T(W_C^* - \tilde{W}_C)) \\ &\quad + k_G \|r\| tr(\tilde{W}_G^T(W_G^* - \tilde{W}_G)) \\ &\quad + k_F \|r\| tr(\tilde{W}_F^T(W_F^* - \tilde{W}_F)) \\ &\quad + r^T\varepsilon + r^T\tau_d + r^T\xi\end{aligned} \tag{22}$$

According to the definition of the Frobenius norm, we can obtain

$$\begin{aligned}tr(\tilde{W}^T(W^* - \tilde{W})) &= \left\langle \tilde{W}, W^* \right\rangle_F - \left\|\tilde{W}\right\|_F^2 \\ &\le \left\|\tilde{W}\right\|_F \|W^*\|_F - \left\|\tilde{W}\right\|_F^2\end{aligned} \tag{23}$$

where $\|\cdot\|_F$ is the Frobenius norm.
Using (23) and considering the boundedness of W^*, ε, τ_d and the definition of ξ, (22) can be deduced as follows

$$\begin{aligned}\dot{V} &\le -\lambda_{\min}(K_v)\|r\|^2 \\ &\quad + k_M \|r\| \left\|\tilde{W}_M\right\|_F (W_{M\max} - \left\|\tilde{W}_M\right\|_F) \\ &\quad + k_C \|r\| \left\|\tilde{W}_C\right\|_F (W_{C\max} - \left\|\tilde{W}_C\right\|_F) \\ &\quad + k_G \|r\| \left\|\tilde{W}_G\right\|_F (W_{G\max} - \left\|\tilde{W}_G\right\|_F) \\ &\quad + k_F \|r\| \left\|\tilde{W}_F\right\|_F (W_{F\max} - \left\|\tilde{W}_F\right\|_F)\end{aligned} \tag{24}$$

where $\lambda_{\min}(K_v)$ is the minimum eigenvalue of K_v.
Thus, when

$$\|r\| > \frac{k_M W_{M\max}^2 + k_C W_{C\max}^2 + k_G W_{G\max}^2 + k_F W_{F\max}^2}{4\lambda_{\min}(K_v)} \tag{25}$$

holds, we get $\dot{V} < 0$. As a result, the convergence condition of the error can be given as (25).

IV. Simulation Results

The performance of the proposed control strategy will be verified by using Matlab/Simulink platform. The system parameters are selected as $m_1 = 15.2$kg, $m_2 = 12.51$kg, $l_1 = 0.42$m, $l_2 = 0.41$m. The parameters with respect to the control scheme are set as $K_v = diag(50, 50)$, $\Gamma_M = diag(5, 5)$, $\Gamma_C = \Gamma_G = \Gamma_F = diag(10, 10)$, $\Lambda = diag(10, 10)$, $\delta = 0.2$, $\rho_d = 0.1$, $k_M = k_C = k_G = k_F = 0.01$. For each RBF neural network, there is one hidden layer and one output layer. The initial weight values of the network is chosen as zero. The number of nodes in the hidden layer is set as 5. The parameters of hidden layer Gaussian functions are designed as $\mu = \begin{bmatrix} -2 & -1 & 0 & 1 & 2 \\ -2 & -1 & 0 & 1 & 2 \end{bmatrix}$, $\sigma_i = 4$ $(i = 1, 2, \cdots, 5)$. The external disturbance is selected as $\tau_d = \begin{bmatrix} 0.2\sin(t) & 0.2\sin(t) \end{bmatrix}^T$. We choose the desired trajectory as the treadmill movement which is a common and effective rehabilitation exercise in clinic. Based on the data in [24], the range of the normal gait speed is from 67 ± 3 to 154 ± 11 steps per minute and the general gait is 100 ± 1 steps per minute. By considering patients' injury condition, the treadmill movement period is set as 4s and the radius of treadmill is selected as 0.1m. Thus, the desired trajectory of the end-point can be expressed as

$$x = \begin{bmatrix} x_1 \\ x_2 \end{bmatrix} = \begin{bmatrix} 0.63 + 0.1\cos(0.5\pi t) \\ 0.1\sin(0.5\pi t) \end{bmatrix}$$

where x is the desired position coordinate of the end-point trajectory in Cartesian space.

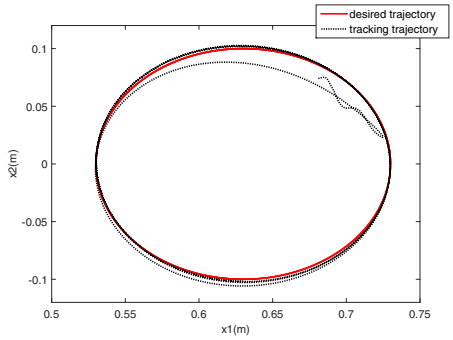

Fig. 5. Trajectory tracking in end-point Cartesian space

Under the condition that $q_{d2} < 0$, the desired trajectory of each joint can be expressed as follows

$$q_d = \begin{bmatrix} q_{d1} \\ q_{d2} \end{bmatrix} = \begin{bmatrix} \arctan\frac{x_2}{x_1} + \arccos\frac{x_1^2+x_2^2+l_1^2-l_2^2}{2l_1\sqrt{x_1^2+x_2^2}} \\ -\arccos(\frac{x_1^2+x_2^2-l_1^2-l_2^2}{2l_1 l_2}) \end{bmatrix}$$

where q_{d1} is the desired angular position coordinates of joint 1, q_{d2} is the desired angular position coordinates of joint 2.
The Jacobian matrix can be written as

$$J = \begin{bmatrix} -l_1\sin q_{d1} - l_2\sin(q_{d1}+q_{d2}) & -l_2\sin(q_{d1}+q_{d2}) \\ l_1\cos q_{d1} + l_2\cos(q_{d1}+q_{d2}) & l_2\cos(q_{d1}+q_{d2}) \end{bmatrix}$$

Thus, the desired angular velocity of each joint can be obtained as

$$\dot{q}_d = J^{-1}\dot{x}$$

In Figs. 5-7, the solid line is the desired motion curve and the dotted line is the actual motion curve of the whole system. After a short adaptation phase, the tracking error is almost less than 0.005 rad and 0.008 rad/s for position and velocity, respectively. Therefore, the proposed control scheme can guarantees a high performance in trajectory tracking under the external disturbance and human voluntary participation. The applied torques at each joint is shown in Fig. 8, respectively. The black line represents the actual

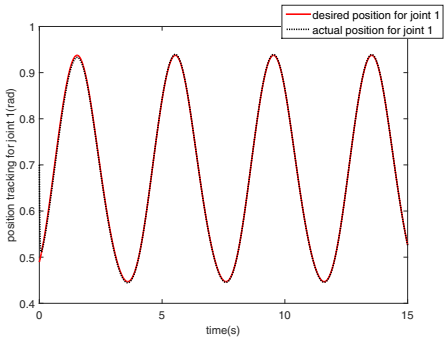

(a) Angular position tracking for joint 1

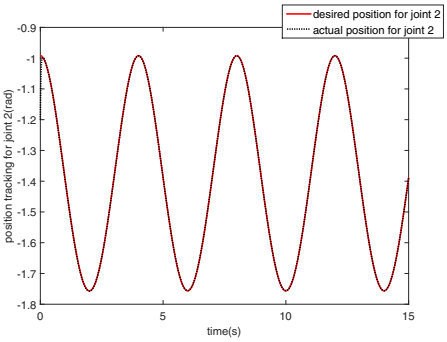

(b) Angular position tracking for joint 2

Fig. 6. Angular position tracking

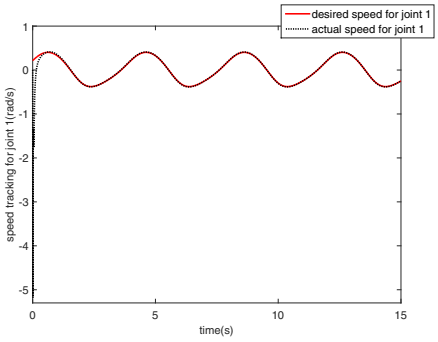

(a) Angular velocity tracking for joint 1

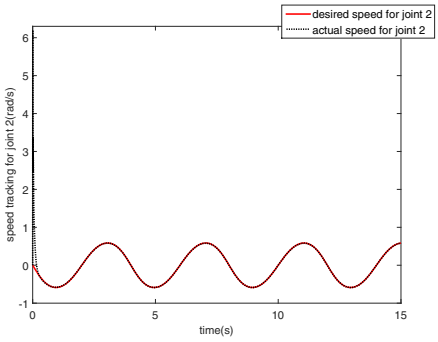

(b) Angular velocity tracking for joint 2

Fig. 7. Angular velocity tracking

output torque. The red line and blue line denote human torque and robot torque, respectively. From Fig. 8, we can be clearly see that the robot works in the assistive mode and the robot torque changes with the variation of human torque. It implies that the robot can change the magnitude or direction of the motor torque to adapt to the patient's different voluntary efforts. During rehabilitation, the robot's operation mode can be switched based on the patient's voluntary torque. The robot will run in the assistive mode when the patient can not catch up with the desired trajectory. In contrast, if the patient moves too fast, the robot will operate in the resistive mode for the sake of security.

V. Conclusions

This paper proposed a control method based on the RBF neural networks for a lower limb rehabilitation robot designed at our laboratory. There is no particular prior knowledge of the system dynamics except the model structure information which is universally valid in robotics. The Lyapunov theory has been used to analyze the stability of the whole system and to deduce the adaptive update rule of the network weights. The simulation result indicates that the proposed control strategy can ensure small tracking errors and possess good robustness to the modeling errors and external disturbance. Using the proposed control scheme, the robot can change its mode to adaptively conduct the rehabilitation training by detecting the human voluntary torque. For future works, we are going to popularize this method to more diverse multi-joint coordination motion modes such as

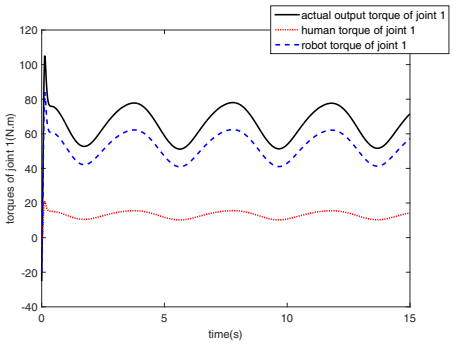

(a) Applied torques on joint 1

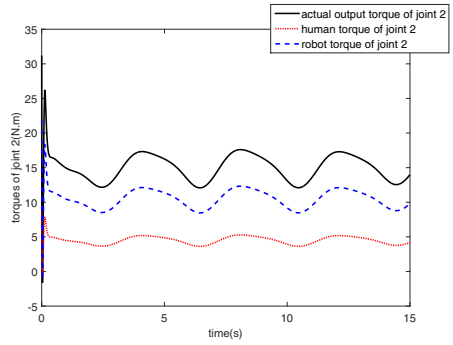

(b) Applied torques on joint 2

Fig. 8. Applied torques of the system

various frequencies and non-periodic motions and the control schemes will be validated in practice.

REFERENCES

[1] D. Bourbonnais and S. V. Noven, "Weakness in patients with hemiparesis," *American Journal of Occupational Therapy*, vol. 43, no. 5, pp. 313–319, 1989.

[2] K. Ito, T. Shioyama, and T. Kondo, "Lower-limb joint torque and position controls by functional electrical stimulation," *Complex Medical Engineering*, pp. 239–249, 2007.

[3] J. E. Pratt, B. T. Krupp, C. J. Morse, and S. H. Collins, "The roboknee: an exoskeleton for enhancing strength and endurance during walking," in *Proceedings of 2004 IEEE International Conference on Robotics and Automation*, 2004, pp. 2430–2435.

[4] F. Reynard, F. Gerber, C. Favre, and A. Al-Khodairy, "Movement analysis with a new robotic device ł the motionmaker^{TM}: A case report," *Gait & Posture*, vol. 30, pp. S149–S150, 2009.

[5] R. Riener, L. Lünenburger, I. Maier, G. Colombo, and V. Dietz, "Locomotor training in subjects with sensori-motor deficits: an overview of the robotic gait orthosis lokomat," *Journal of Healthcare Engineering*, vol. 1, no. 2, pp. 197–216, 2010.

[6] H. Watanabe, N. Tanaka, T. Inuta, H. Saitou, and H. Yanagi, "Locomotion improvement using a hybrid assistive limb in recovery phase stroke patients: a randomized controlled pilot study," *Archives of physical medicine and rehabilitation*, vol. 95, no. 11, pp. 2006–2012, 2014.

[7] S. Mefoued, "A robust adaptive neural control scheme to drive an actuated orthosis for assistance of knee movements," *Neurocomputing*, vol. 140, pp. 27–40, 2014.

[8] S. Mefoued, S. Mohammed, and Y. Amirat, "Toward movement restoration of knee joint using robust control of powered orthosis," *IEEE Transactions on Control Systems Technology*, vol. 21, no. 6, pp. 2156–2168, 2013.

[9] S. Kim and J. Bae, "Development of a lower extremity exoskeleton system for human-robot interaction," in *Proceedings of 2014 International Conference on Ubiquitous Robots and Ambient Intelligence*, 2014, pp. 132–135.

[10] T. Madani, B. Daachi, and K. Djouani, "Adaptive controller based on uncertainty parametric estimation using backstepping and sliding mode techniques: application to an active orthosis," in *Proceedings of 2014 European Control Conference*, 2014, pp. 1869–1874.

[11] L. Cheng, Z.-G. Hou, and M. Tan, "Adaptive neural network tracking control of manipulators using quaternion feedback," in *Proceedings of 2008 IEEE International Conference on Robotics and Automation*, 2008, pp. 3371–3376.

[12] L. Cheng, Z.-G. Hou, M. Tan, and H. Wang, "Adaptive neural network tracking control for manipulators with uncertainties," in *Proceedings of the 17th IFAC world congress*, 2008, pp. 2382–2387.

[13] L. Cheng, Z.-G. Hou, and M. Tan, "Adaptive neural network tracking control for manipulators with uncertain kinematics, dynamics and actuator model," *Automatica*, vol. 45, no. 10, pp. 2312–2318, 2009.

[14] L. Cheng, Y. Lin, Z.-G. Hou, M. Tan, J. Huang, and W. Zhang, "Adaptive tracking control of hybrid machines: a closed-chain five-bar mechanism case," *IEEE/ASME Transactions on Mechatronics*, vol. 16, no. 6, pp. 1155–1163, 2011.

[15] X.-L. Xie, Z.-G. Hou, L. Cheng, C. Ji, M. Tan, and H. Yu, "Adaptive neural network tracking control of robot manipulators with prescribed performance," *Proceedings of the Institution of Mechanical Engineers, Part I: Journal of Systems and Control Engineering*, vol. 225, no. 6, pp. 790–797, 2011.

[16] Q. Xu, "Piezoelectric nanopositioning control using second-order discrete-time terminal sliding mode strategy," *IEEE Transactions on Industrial Electronics*, in press, DOI 10.1109/TIE.2015.2449772, 2015.

[17] Q. Xu, "Digital sliding mode prediction control of piezoelectric micro/nanopositioning system," *IEEE Transactions on Control Systems Technology*, vol. 23, no. 1, pp. 297–304, 2015.

[18] F. Zhang, P. Li, Z. Hou, X. Xie, Y. Chen, Q. Li, and M. Tan, "An adaptive rbf neural network control strategy for lower limb rehabilitation robot," in *Proceedings of the Intelligent Robotics and Applications*, 2010, pp. 417–427.

[19] Y. Chen, J. Hu, L. Peng, and Z.-g. Hou, "The fes-assisted control for a lower limb rehabilitation robot: simulation and experiment," *Robotics and Biomimetics*, vol. 1, no. 1, pp. 1–20, 2014.

[20] H. K. Khalil, *Nonlinear control*. Prentice Hall, 2014.

[21] S. S. Ge, C. C. Hang, T. H. Lee, and T. Zhang, *Stable adaptive neural network control*. Springer Science & Business Media, 2013.

[22] L. Cheng, W. Liu, Z.-G. Hou, J. Yu, and M. Tan, "Neural network based nonlinear model predictive control for piezoelectric actuators," *IEEE Transactions on Industrial Electronics*, in press, DOI: 10.1109/TIE.2015.2455026, 2015.

[23] F. L. Lewis, D. M. Dawson, and C. T. Abdallah, *Robot manipulator control: theory and practice*. CRC Press, 2003.

[24] M. D. Latt, H. B. Menz, V. S. Fung, and S. R. Lord, "Walking speed, cadence and step length are selected to optimize the stability of head and pelvis accelerations," *Experimental Brain Research*, vol. 184, no. 2, pp. 201–209, 2008.